Chapter 3

Interaction of radiation with matter

3.1 Types of radiation

Interaction of radiation with the matter is necessary in order to characterize the microstructures:

- photons
- electrons
- neutrons
- protons
- ions/atoms

The penetration depth or mean free path of the incident beam determines the depth and volume of material that will be sampled. In many cases one is probing with one type of radiation but detecting a second type. This occurs in X-ray photoelectron spectroscopy (XPS) where the incident probe is a beam of X-ray photons but emitted electrons are detected,whereas this is reversed for the technique of energy dispersive X-ray(EDX) analysis. Generally the particle or radiation which has the shortest mean free path in the material will determine the volume analysed. Whatever beam is selected we must be aware of its interaction with the material, what photons, electrons or other particles are ejected and how they, in turn, inter-act with the material. Only in this way can we use the emitted signals to gain an understanding of the material being examined. The material can be damaged by this interaction:

- surface observations ⇒visible light is bombarding the surface (damage to the photographic layer)
- for a higher magnification ⇒ electrons with energies between 10–30 keV (greater penetration and consequently greater damage)
- high resolution and high sensitivity ⇒ high energy ions (visible damage)

It is necessary to choose the right method due to their damage characteristics.

3.2 Photon interactions

The electromagnetic radiation can interact with electrons or phonons. Photons are discrete quanta of electromagnetic radiation. The photon is identified by the wavelength, λ, energy, E, and frequency, ν , all of which are related by the equation

$$h\nu = E = hc/\lambda \tag{3.1}$$

where h is the Planck constant and c the velocity if light.The electromagnetic spectrum spans a vast range with wavelengths varying from 10^6 m down to 10^{-14} m. If we are to use electro-magnetic radiation for microstructural characterisation of materials a photon wavelength is needed that is of comparable size to the features being studied. This means that photon wavelengths greater than 10^{-4}m would result in an inadequate spatial resolution and we do not require radiation less than about 10^{-10} m.
The penetration of photons shows considerable and dramatic variations between different types of material and photon energy or wavelength. It is not possible or instructive to go into any detail regarding penetration depths over the whole of the electromagnetic spectrum, but only some specific wavelengths that are important for interrogating the microstructure of materials. The long wavelength infrared radiation is used to characterise materials by determining how specific wavelengths are absorbed, visiblelight is used in a variety of instruments mainly to obtain a visual image of the surface while at the shorter wavelength ultraviolet radiation is often used to obtain information concerning the electron distribution in the surface atoms. Some materials are opaque while others are transparent to this range of wavelengths. However, even the most opaque or highly reflecting of these materials will allow the radiation to penetrate at least a fraction of a wavelength below the surface. In the case of visible light, where the wave-length is approximately 500 nm this penetrates an average of between 50 to 300 nm into the bulk so that any analysis performed or image obtained will average over several hundred atom layers.

3.2.1 Very short wavelengths ($< 10^{-12}$ m, γ-rays)

The method that uses γ-rays to characterize materials is called *Mössbauer spectroscopy.*

Key to the success of the technique is the discovery of recoilless γ-ray emission and absorption, now referred to as the *Mössbauer effect*, after its discoverer Rudolph Mössbauer, who first observed the effect in 1957 and received the Nobel Prize in Physics in 1961 for his work.

Mössbauer effect

Nuclei in atoms undergo a variety of energy level transitions, often associated with the emission or absorption of a gamma ray. These energy levels are influenced by their surrounding environment, both electronic and magnetic, which can change or split these energy levels. These changes in the energy levels can provide information about the atom's local environment within a system and ought to be observed using resonance-fluorescence. There are, however, two major obstacles in obtaining this information:

- the 'hyperfine' interactions between the nucleus and its environment are extremely smaller,

- the recoil of the nucleus as the gamma-ray is emitted or absorbed prevents resonance.

Just as a gun recoils when a bullet is fired, conservation of momentum requires a free nucleus (such as in a gas) to recoil during emission or absorption of a gamma ray.

- If a nucleus at rest emits a gamma ray, the energy of the gamma ray is slightly less than the natural energy of the transition (difference is equal to the recoil energy E_R),
- but in order for a nucleus at rest to absorb a gamma ray, the gamma ray's energy must be slightly greater than the natural energy.

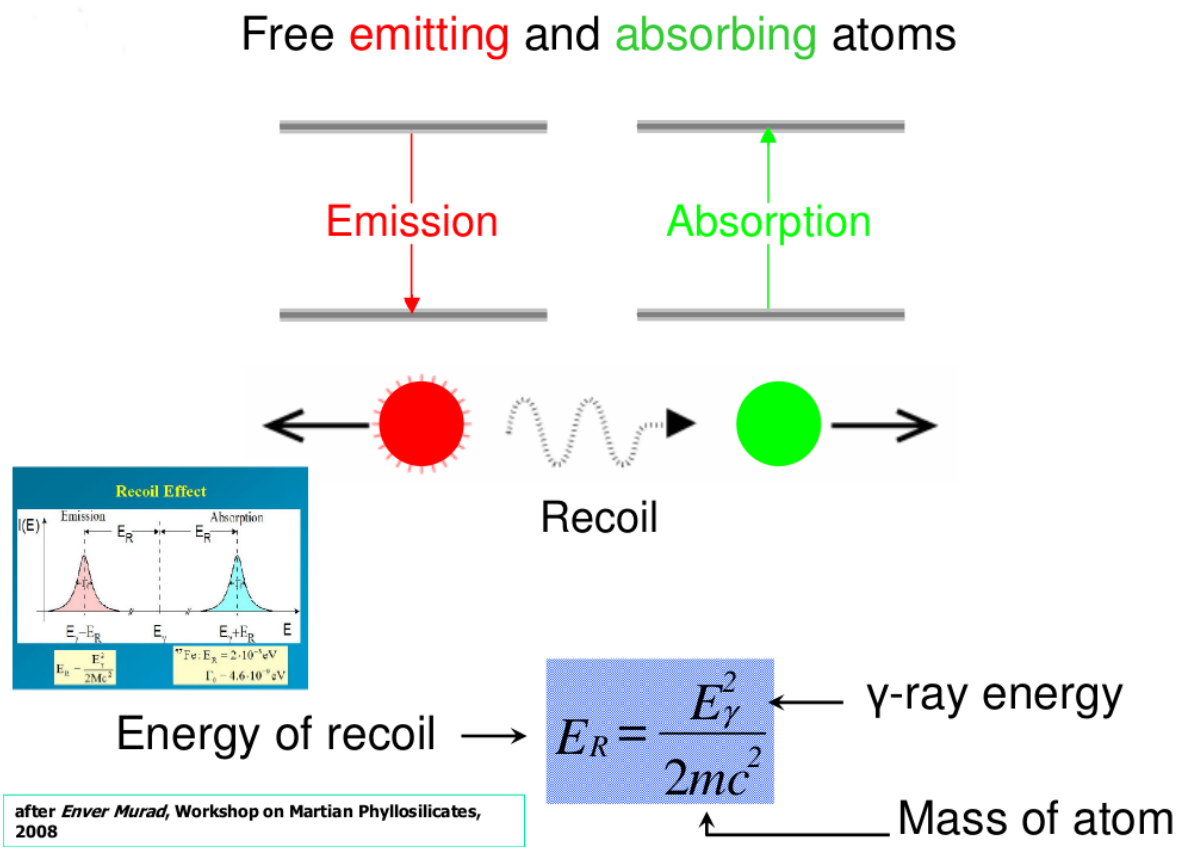

Figure 3.1: Recoil of free nuclei in emission or absorption of a gamma-rays

This means that nuclear resonance (emission and absorption of the same gamma ray by identical nuclei) is unobservable with free nuclei, because the shift in energy is too great and the emission and absorption spectra have no significant overlap.

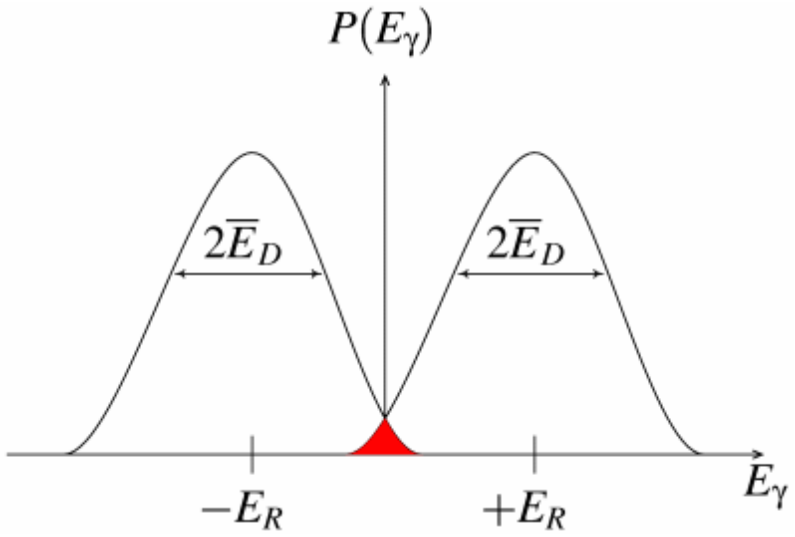

Figure 3.2: Resonant overlap in free atoms. The overlap shown shaded is greatly exaggerated.

In order to achieve resonance in emission and absorption the loss of the recoil energy must be overcome in some way.

Nuclei in a solid crystal are not free to recoil because they are bound in place in the crystal lattice. When a nucleus in a solid emits or absorbs a gamma ray, some energy can still be lost as recoil energy, but in this case it always occurs in discrete packets called phonons (quantized vibrations of the crystal lattice). Any whole number of phonons can be emitted, including zero, which is known as a "recoil-free" event. In this case conservation of momentum is satisfied by the momentum of the crystal as a whole, so practically no energy is lost.

Mössbauer found that a significant fraction of emission and absorption events will be recoil-free, which is quantified using the Lamb–Mössbauer factor. This fact is what makes Mössbauer spectroscopy possible, because it means gamma rays emitted by one nucleus can be resonantly absorbed by a sample containing nuclei of the same isotope, and this absorption can be measured.

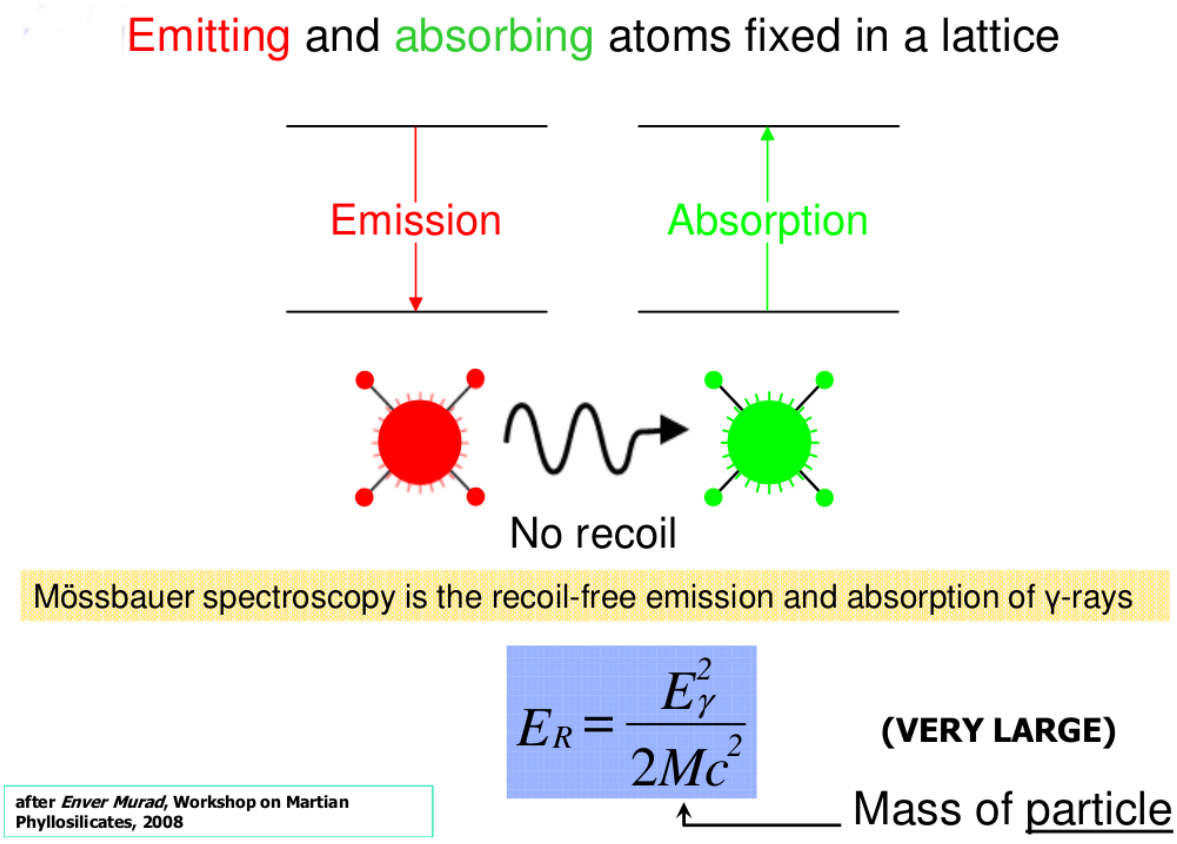

Figure 3.3: Atoms fixed in lattice.

In its most common form, Mössbauer absorption spectroscopy,

- a solid sample is exposed to a beam of gamma radiation,
- and a detector measures the intensity of the beam transmitted through the sample.

The atoms in the source emitting the gamma rays must be of the same isotope as the atoms in the sample absorbing them.

If the emitting and absorbing nuclei were in identical chemical environments, the nuclear transition energies would be exactly equal and resonant absorption would be observed with both materials at rest. *The difference in chemical environments, however, causes the nuclear energy levels to shift in a few different ways.* Although these energy shifts are tiny (often less than a micro-electronvolt), the extremely narrow spectral linewidths of gamma rays for some radionuclides make the small energy shifts correspond to large changes in absorbance. To bring the two nuclei back into resonance it is necessary *to change the energy of the gamma ray slightly*, and in practice this is always done using the *Doppler effect.*

During Mössbauer absorption spectroscopy, the source is accelerated through a range of velocities using a linear motor to produce a Doppler effect and scan the gamma ray energy through a given range. A typical range of velocities for 57Fe, for example, may be ±11 mm/s (1 mm/s = 48.075 neV).

In the resulting spectra, gamma ray intensity is plotted as a function of the source velocity. At velocities corresponding to the resonant energy levels of the sample, a fraction of the gamma rays are absorbed, resulting in a drop in the measured intensity and a corresponding dip in the spectrum. The number, positions, and intensities of the dips (also called peaks; dips in transmitted intensity are peaks in absorbance) provide information about the chemical environment of the absorbing nuclei and can be used to characterize the sample.

Mössbauer spectroscopy is limited by the need for a suitable gamma-ray source. Usually, this consists of a radioactive parent that decays to the desired isotope. For example,

- the source for 57Fe consists of 57Co, which decays by electron capture to an excited state of 57Fe,
- then subsequently decays to a ground state emitting the desired gamma-ray.
- The radioactive cobalt is prepared on a foil, often of rhodium.

Ideally the parent isotope will have a sufficiently long half-life to remain useful, but will also have a sufficient decay rate to supply the required intensity of radiation.

Mössbauer spectroscopy has an extremely fine energy resolution and can detect even subtle changes in the nuclear environment of the relevant atoms. Typically, there are three types of nuclear interactions that are observed

- isomer shift (or chemical shift) - is a relative measure describing a shift in the resonance energy of a nucleus due to the transition of electrons within its s orbital. The whole spectrum is shifted in either a positive or negative direction depending upon the s electron charge density. This change arises due to alterations in the electrostatic response between the non-zero probability s orbital electrons and the non-zero volume nucleus they orbit.

- quadrupole splitting - reflects the interaction between the nuclear energy levels and surrounding electric field gradient (EFG). Nuclei in states with non-spherical charge distributions, i.e. all those with angular quantum number (I) greater than 1/2, produce an asymmetrical electric field which splits the nuclear energy levels. This produces a nuclear quadrupole moment.

Figure 3.4: Chemical shift and quadrupole splitting of the nuclear energy levels and corresponding Mössbauer spectra

- hyperfine splitting (or Zeeman splitting) - is a result of the interaction between the nucleus any surrounding magnetic field. A nucleus with spin, I, splits into 2I + 1 sub-energy levels in the presence of magnetic field. For example, a nucleus with spin state I= 3/2 will split into 4 non-degenerate sub-states with mI values of +3/2, +1/2, -1/2 and −3/2. Each split is hyperfine, being in the order of 10^{-7}eV. The restriction rule of magnetic dipoles means that transitions between the excited state and ground state can only occur where mI changes by 0 or 1. This gives six possible transitions for a 3/2 to 1/2 transition.

Figure 3.5: Magnetic splitting of the nuclear energy levels and the corresponding Mössbauer spectrum

3.2.2 Short wavelengths ($10^{-12} to 10^{-9}$ m, including X-rays and ultraviolet)

If photon has enough energy to excite electron to high energy levels, two effects can occur:

- **internal photoeffect** (e.g. photoconductivity)
- **external photoeffect** or the photoemission.

The kinetic energy is:

$$\frac{1}{2}mv^2 = E_{\mathrm{F}} \pm \delta E - E_{\mathrm{af}} + h\nu - \Delta E. \tag{3.2}$$

At 0 K the kinetic energy is maximum

$$(\frac{1}{2}mv^2)_{\max} = h\nu - (E_{\mathrm{af}} - E_{\mathrm{F}}) = h\nu - \chi = h(\nu - \nu_0), \tag{3.3}$$

where ν_0 is the frequency of photoelectric effect.

In the case of photoemission induced absorption (**X-ray**), the photon has enough energy to excite an electron from some inner layers of solid.

$$\frac{1}{2}mv^2 = h\nu - \chi - E_{\mathrm{B}}, \tag{3.4}$$

where E_{B} is the binding energy of the inner layers. The binding energy is characteristic for each substance, so the kinetic electrons emitted bear information related to the electronic structure and thus, the type of material.

3.2.3 Fowler‘s theory for metal/vacuum interfaces

Fowler proposed a theory in 1931 which showed that the photoelectric current variation with the light frequency could be accounted for by the effect of temperature in the number of electrons available for emission, in accordance with the distribution law of Sommerfeld‘s theory for metals. Sommerfeld‘s theory had resolved some of the problems surrounding the original models for electron in metals. In classical Drude theory, a metal had been envisaged as a three-dimensional potential well (box) containing a gas of freely mobile electrons. This adequately explained their high electrical and thermal conductivities. However, because experimentally it was found that metallic electrons do not show a gas-like heat capacity, the Boltzman distribution law is inappropriate. A Fermi-Dirac distribution function is required, consistent with the need that the electrons obey the Pauli exclusion principle and this distribution function has the form

$$P(E) = \frac{1}{1 + exp[(E - E_F)/kT]} \tag{3.5}$$

At ordinary temperatures, the Fermi energy $E_F \gg kT$. Fowler‘s law, referred to above as the "square law", is readily tested in practice since it predicts at T=0 K

$$i \propto (\nu - \nu_0)^2 \tag{3.6}$$

where ν_0 is the photoelectric threshold frequency and ν refers to a range of energies from threshold to a few kT above threshold. To a good approximation, the photoelectric yield per unit light intensity near ν_0 is proportional simply to the number of electrons incident per unit time. The energy condition can be written

$$(1/2m)p^2 + h\nu > \phi \tag{3.7}$$

where p is the initial momentum of the electron normal to the surface. The escaping electrons have been termed the "available electrons".
Fowler‘s derivation for the single photon does not explicitly involve the quantum mechanical form of current; instead, a semi-classical flux of electrons arriving at the metal surface is used. The electron gas in the metal will obey Fermi-Dirac statistics, and the number of electrons per unit volume having velocity components in the ranges $u, u+du, \nu, \nu+d\nu$ and $w+dw$ is given by the formula

$$n(u,\nu,w)dud\nu dw = 2(\frac{m}{h})^2 \frac{dud\nu dw}{1+exp[\frac{1}{2}m(u^2+\nu^2+w^2)-E_F]/kT} \tag{3.8}$$

where u is the velocity normal to the surface and m is the electron mass. The number of electrons per volume, $n(u)du$, with their velocity component normal to the surface in the range $u, u+du$ is given by:

$$n(u)du = \frac{4\pi kT}{m}(\frac{m}{h})^3 \log[1+\exp(E_F - \frac{1}{2}mu^2)/kT]du \tag{3.9}$$

The solution for the photoelectric current resulted in the form

$$i \propto \frac{(h\nu-\phi)^{3/2}}{(\phi_0-h\nu)^{1/2}}. \tag{3.10}$$

A method for determining the threshold frequency of the illuminated surface ν_0 is that which makes use of the complete photoelectric emission. When a metal surface is exposed to the total thermal radiation from a black body with a temperature T, the total photoelectric current is given by:

$$i = A‘T^2 e^{-\frac{h\nu_0}{kT}} \tag{3.11}$$

were $A‘$ is a constant.

3.2.4 Measurement of the photoelectric work function

- Fowler isotherm: measurement of the photocurrent depending on the frequency of incident radiation at constant temperature, the $\ln i_\mathrm{f}/T^2$ is expressed as $h\nu/kT$ and compared with the theoretical curve

$$\ln\frac{i_\mathrm{f}}{T^2} = \ln(\alpha A_0) + \ln f(x) = B + \Phi[\frac{h}{kT}(\nu-\nu_0)]. \tag{3.12}$$

  From the Fowler equation, giving the relation between temperature and photoelectric emission, ν_0 can be determinate by plotting the $\ln f(\Delta)$ as a function of Δ. A universal curve is obtained. Then $\ln\frac{i}{T^2}$ is plotted against $\frac{h\nu}{kT}$. A curve us obtained of the same shape as the universal curve, which can be made to coincide with it by a parallel shift. The vertical shift is measure of B, the horizontal is equal to $\frac{h\nu_0}{kT}$.

- duBridge isochromatic method: measurements at one frequency ν but different temperatures. For this purpose $\ln f(\Delta)$ is plotted against $\ln|\Delta|$, and again a universal curve is obtained. From the experimental data $\ln i_\mathrm{f}/T^2$ is plotted against $\ln 1/T$. For different frequencies the temperature dependence of the photoemission differs
- for $\nu = \nu_0$ is $i_\mathrm{f} = \alpha A_0 = \pi^2/12T^2$
- for $x \gg 1$; $\nu > \nu_0$, is $f(x) = \pi^2/6 + x^2/2$ and

$$i_\mathrm{f} = \frac{\alpha A_0}{2}\left[\frac{h^2(\nu-\nu_0)^2}{k^2} + \frac{\pi^2}{3}\right], \tag{3.13}$$

  where the parabolic dependence is applied obly when the first term in the brackets is sufficiently small.
- for $x \ll 1$, $\nu < \nu_0$, is $f(x) = e^x$ and

$$i_\mathrm{f} = \alpha A_0 T^2 \exp(-\frac{h(\nu_0-\nu)}{kT}). \tag{3.14}$$

3.2.5 Interaction of excited electrons with matter

The **hot-electron** problem represents the study of the deviations from the linear response regime due to heating of charge carriers above the thermal equilibrium. Studies have been carried out in 1930s, mainly by Russian physicist Landau and Davidov. This means that electron temperature T_e which , in the presence of an external high electric field, is higher that the lattice temperature T.
Nonlinear transport deals with problems that arise when a sufficiently strong electric field is applied to a semiconductor sample, so that the current deviates from the linear response. This effect is typical of semiconductors and cannot be seen on metals since, owing to their large conductivities, Joule heating would destroy the material before deviations from the linearity could be observed.

Considering

$$v^{(i)}(t) = v_0^{(i)} + a\Delta t^{(i)} \tag{3.15}$$

where $v^{(i)}(t)$ is the instantaneous velocity if the i-th electron at time t, $\Delta t^{(i)}$ is the same time elapsed after its last scattering event, and $a = eE/m$ is the electron acceleration, due to a constant and uniform applied electric field E. The region of field strengths where transport starts to deviate from linearity is called **warm-electron region**.

3.2.6 Photoemission from semiconductors

There are some differences when we speak about the photoemission from metals and semiconductors. All high quantum yield photocathodes are semiconductor ones. The absorption of light is affected by:

- internal absorption due to their band gap

- external absorption from the external layer

The Fermi level is influenced by the surface layers and the type of semiconductor used. Electron coming from different depths have different space charge and work function ⇒ as they would have different work function for different photoelectrons excited at different wavelengths.
The density of stated around Fermi level increases strongly and we cannot assume that photon absorption is independent from electron's energy state. The quantum yield increases with the temperature faster than in metals.

3.2.7 Photocathode

- IR region: Ag-O-Cs, also called S-1. This was the first compound photocathode material, developed in 1929. Sensitivity from 300 nm to 1200 nm. Since Ag-O-Cs has a higher dark current than more modern materials photomultiplier tubes with this photocathode material are nowadays used only in the infrared region with cooling.

- visible region: Sb-Cs has a spectral response from UV to visible and is mainly used in reflection-mode photocathodes. and also bi-alkali (antimony-rubidium-caesium Sb-Rb-Cs, antimony-potassium-caesium Sb-K-Cs). Spectral response range similar to the Sb-Cs photocathode, but with higher sensitivity and lower dark current than Sb-Cs. They have sensitivity well matched to the most common scintillator materials and so are frequently used for ionizing radiation measurement in scintillation counters.

- UV region: metals and Cs-Te (Cs-I). These materials are sensitive to vacuum UV and UV rays but not to visible light and are therefore referred to as solar blind. Cs-Te is insensitive to wavelengths longer than 320 nm, and Cs-I to those longer than 200 nm.

3.2.8 Interaction of matter with very long wavelengths photons ($\geq 1mm$) - including radio and microwaves

All nucleons, that is neutrons and protons, composing any atomic nucleus, have the intrinsic quantum property of spin. The overall spin of the nucleus is determined by the spin quantum number I. Some nuclei have integral spins (e. g. $I = 1, 2, 3 \ldots$), some have fractional spins (e.g. $I = 1/2, 3/2, 5/2....$), and a few have no spin, $I = 0$ (e.g. 12C, 16O, 32S, ...). Isotopes of particular interest and use to organic chemists are 1H, 13C, 19F and 31P, all of which have I = 1/2.

A non-zero spin is always associated with a non-zero magnetic moment μ

$$\mu = \gamma S \tag{3.16}$$

where γ is the gyromagnetic ratio.

It is this magnetic moment that allows the observation of nuclear magnetic resonance (NMR) absorption spectra caused by transitions between nuclear spin levels in the presence of external magnetic field (spin states splitting).

`http://www2.chemistry.msu.edu/faculty/reusch/VirtTxtJml/Spectrpy/nmr/nmr1.htm`

Electron spin resonance (ESR) or *electron paramagnetic resonance (EPR)* is a related technique in which transitions between electronic spin levels are detected rather than nuclear ones. The basic

principles are similar but the instrumentation, data analysis, and detailed theory are significantly different. Moreover, there is a much smaller number of molecules and materials with unpaired electron spins that exhibit ESR absorption than those that have NMR absorption spectra. ESR has much higher sensitivity than NMR does.

3.3 Electron interactions

- desorption of neutral particles
- excitation of photons (x-ray, chatodoluminescence)
- reality of material: cleaning, activation energy for chemical and physical processes, electron lithography
- change of material
- emission of electrons: (a) without interaction, (b) elastic scattering (diffraction on passage), (c) elastic reflection (diffraction on reflection), (d) inelastic reflection (characteristic energy loss), (e) backscatter electron, (f) electron transmission with the possibility to emit others and (g) electron transmission with secondary electron emission.
  When a sample is bombarded with charged particles, the strongest region of the electron energy spectrum is due to secondary electrons. The secondary electron yield depends on many factors, and is generally higher for high atomic number targets, and at higher angles of incidence. There is a lot of information in this secondary electron "background", but, unlike Auger and other electron spectroscopies, it is not directly chemical or surface specific in general.
  Total electron current from a substance is the **current of secondary electrons** on reflection or transmission.

3.3.1 Electron emission

The ration between this current I_s and primary I_p is called **secondary emission coefficient** $\sigma = I_\mathrm{s}/I_\mathrm{p}$. By selecting the secondary electrons by their energies we can identify individual interactions:

- the highest maximum of primary energy level $\Rightarrow$ elastic reflection of e^-
  interaction with the atom like a whole, there is no change in energy but, the electron momentum can be changed dramatically. For electron energy higher than ($\geq$ 5 keV)the effect is called Rutherford Backscattering (RBS)

$$\frac{dQ(\theta)}{d\Omega} = \frac{1}{4}\left(\frac{e^2\ (Z - F(\theta))}{4\pi\epsilon_0\ m_\mathrm{red}\ g^2}\right)^2 \frac{1}{\sin^4(\theta/2)}, \tag{3.17}$$

  where $F(\theta)$ is the screening effect of electrons. $F(\theta)$ is insignificant at high angles θ and strong scattering can occur only in heavy atoms (used for TEM contrast). When the target

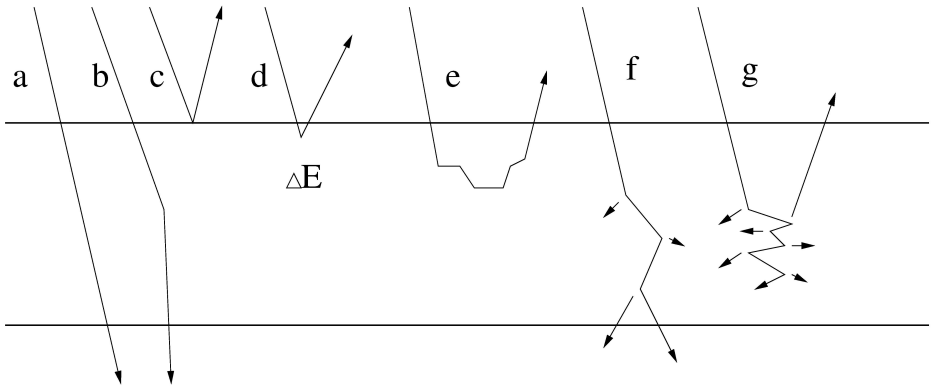

Figure 3.6: Electron interaction with the solid state.

is a crystalline material **diffraction** and **channelling** occurs. When electron scattering from crystal lattice is coherent, amplification in those direction occurs, which is represents **Bragg law**:

$$n\lambda = 2d_{\mathrm{hkl}} \sin\theta, \tag{3.18}$$

where n is a integer d_{hkl} is is the spacing between the planes in the atomic lattice expressed with Miller indexes. This method is used to examine the bulk crystalline structure ($E \approx$ 10 keV) or the surface structure using low-energy electron diffraction (LEED) or very small angle relection in reflection high-energy electron diffraction (RHEED).

- the smaller peaks to the left show the shift in maximum elastic reflection of e^- $\Rightarrow$ electrons which suffer energy losses.
  Electrons undergo a variety of interactions:

- adsorbed molecules are excited on vibrational state $\Delta E \approx$ 50–500 meV;

- individual interaction with valence e^-, $\Delta E \approx$ 3–20 eV but without a sharp peak because the valence band has a width of several eV;

- multiple interactions with the valence e^-which is bombarded by an electron, vibrating with frequency

$$\omega_{\mathrm{p}} = \frac{1}{\epsilon_0} \frac{n_0 e^2}{m} \tag{3.19}$$

for plasmon in volume, or

$$\omega_{\mathrm{s}} = \frac{\omega_{\mathrm{p}}}{\sqrt{1+\epsilon_r}} = \frac{\omega}{\sqrt{2}} \tag{3.20}$$

for excitation of the surface plasmon. ΔE is between 5 and 60 eV.

Inelastic interactions include phonon excitations, inter and intra band transitions, plasmon excitations, inner shell ionizations are studied by **electron energy loss spectroscopy** (EELS).

- smaller peaks which are not shifted by energy ⇒ **Auger** e^- which have for each substance a characteristic position.

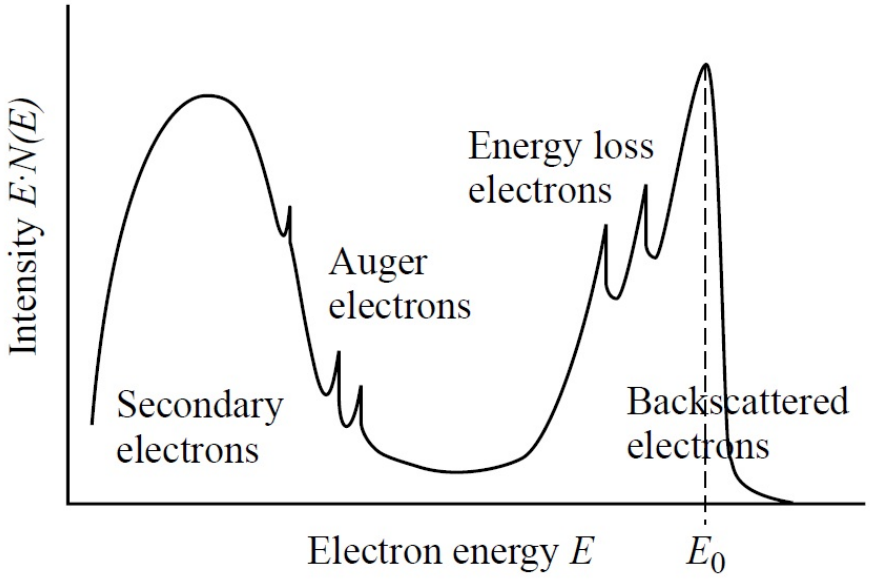

Figure 3.7: Electron energy distribution.

Primary e^- removes a core e^- (e.g. from K shell). The core state electron is removed leaving behind a hole. As this is an unstable state, the core hole can be filled by an outer shell electron, whereby the electron moving to the lower energy level loses an amount of energy equal to the difference in orbital energies. The transition energy can be coupled to a second outer shell electron which will be emitted from the atom if the transferred energy is greater than the orbital binding energy. The Auger energy released

$$E_{\mathrm{k}} = E_{\mathrm{K}} - E_{\mathrm{L}} - E'_{\mathrm{V}} - E_{\mathrm{af}}. \tag{3.21}$$

The E'_{V} is not equal with the original level energy E_{V}, because the e^- on the level V moves in a potential and the e^- on the level L is missing. The Auger requires the existence of at least two energy levels to three electrons. That is why it can not measure H and He. The elements with atomic number between 3 and 14 have KLL line, elements between 14 and 40 have LMM line, between 40 and 79 are MNN line and for heavier elements NOO line exists.

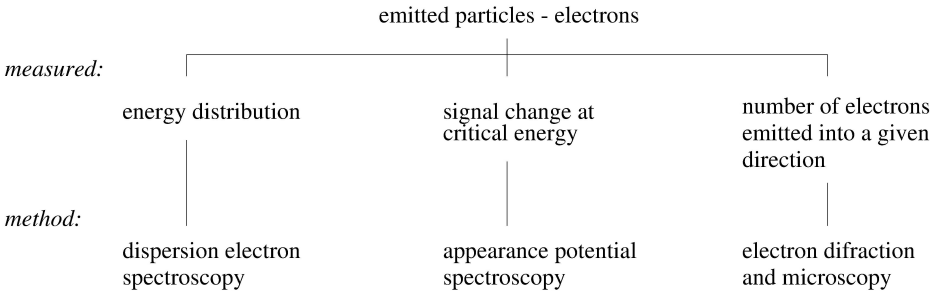

Figure 3.8: Overwiev of measuring methods using emitted electrons.

3.4 Interaction of ions with solid surface

Differences exists in the interaction of ions and electrons with matter. Ions are much heavier, have bigger dimensions and they can have higher charges.

Interakce iontů a atomů s pevnými látkami je základem mnoha technologických procesů materiálového inženýrství, protože může vyústit ve strukturní změny materiálu, implantaci dopadající částice, či k rozprášení pevné látky. Také mnoho metod charakterizace povrchu materiálů je založeno na detekci odražených nebo emitovaných částic při iontovém bombardu. Emitované částice můžou být

- secondary electrons (secondary ion-electron emission),
- photons (characteristic x-rays and visible radiation - ionoluminescence),
- ions (ion scattering, ion-ion secondary emission),
- neutral particles (cathode sputtering),
- products of nuclear reactions

Všechny procesy způsobené dopadem atomu či iontu na pevný materiál jsou schematicky naznačeny na obrázku Fig. 3.9.

Který proces nastane po dopadu atomu či iontu na povrch záleží na mnoha faktorech, jako je energie dopadající částice (E_0), úhel dopadu, tok dopadajících částic (γ_i), hmotnost a atomové číslo dopadající částice (M_1 respektive Z_1), hmotnost a atomové číslo atomů terče (M_2 respektive

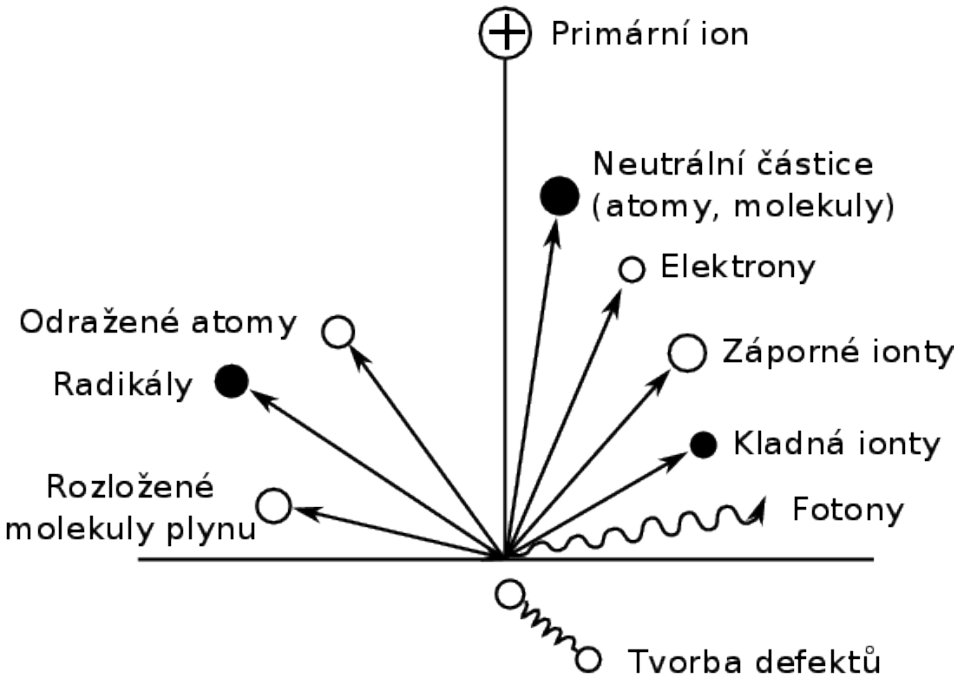

Figure 3.9: Důsledky iontového bombardování.

Z_2) a náboj dopadajících částic a částic terče. Za podmínek obvyklých pro opracovávání materiálů lze interakci projektilu a terče rozdělit na dva odlišné mechanismy

- Jaderné srážky, například elastické srážky atomů
- Elektronické srážky, při nichž jsou excitovaný, nebo emitovány elektrony z materiálu.

3.4.1 Kinematika dvojné srážky

V případě jaderných srážek jsou hmotnosti interagujících částic poměrně blízké. V případě elastické srážky tak může docházet k velké ztrátě kinetické energie dopadající částice, velkému rozptylu dopadající částice a vzniku energetických zpětně odražených atomů. $E_{\mathrm{i},1}$ a E_{t} jsou dány vztahy

$$\begin{aligned} E_1 &= KE_0 \\ E_2 &= (1-K)E_0 \end{aligned} \tag{3.22}$$

kde K je kinetický faktor daný poměrem hmotností M_1/M_2 a úhlem rozptylu v laboratorní soustavě θ. Pokud je hmotnost dopadajícího atomu větší, než hmotnost zasaženého atomu, $M_1/M_2 > 1$, je kinetický faktor daný vztahem:

$$K = \left[\frac{\cos\theta \pm \left({\frac{M_2}{M_1}}^2 - \sin^2\theta \right)^{1/2}}{\frac{M_2}{M_1} + 1} \right]^2 . \tag{3.23}$$

Pokud $M_1/M_2 \leq 1$ výraz se zjednoduší na tvar

$$K = \left[\frac{\cos\theta + \left({\frac{M_2}{M_1}}^2 - \sin^2\theta \right)^{1/2}}{\frac{M_2}{M_1} + 1} \right]^2 . \tag{3.24}$$

Energie předaná zasaženému atomu lze vyjádřit zjednodušením rovnice (3.23) jako

$$E_2 = \frac{4M_1M_2}{(M_1+M_2)^2} \sin^2\frac{\theta_{\mathrm{c}}}{2}\, E_0, \tag{3.25}$$

kde θ_{c} je rozptylový úhel v těžišťové soustavě.

3.4.2 Účinný průřez

Vystavení materiálu proudu atomů, či iontů vede k vzájemné interakci velkého množství částic. Proto je obvyklé popisovat tento děj pomocí pravděpodobnostních veličin, založených na pravděpodobnosti rozptylu částic. Uvažujme částici mířící do bodu ve vzdálenosti b od středu jiné částice. Schéma odklonění této částice je na obrázku 3.10.

Veličina b je jeden ze srážkových parametrů, tzv. záměrná vzdálenost. Tok částic bude značen Γ. Částice vstupující do srážky z diferenciální oblasti $b\,db\,d\phi_{\mathrm{i}}$ opouštějí s určitou pravděpodobností

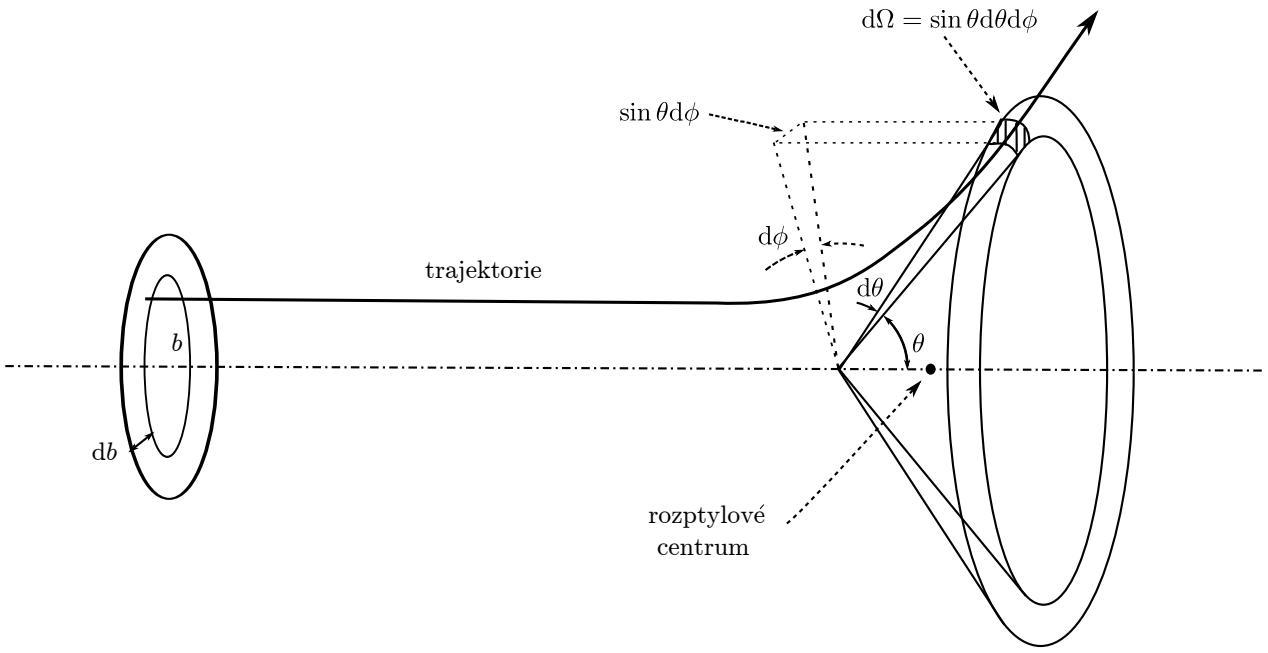

Figure 3.10: Schéma rozptylu lehké částice

srážku skrze diferenciální prostorový úhel Ω definovaný pomocí rozptylového úhlu θ_i a orientace roviny srážky ϕ_i jako

$$\mathrm{d}\Omega = \sin\theta_\mathrm{i}\mathrm{d}\theta_\mathrm{i}\mathrm{d}\phi_\mathrm{i}. \tag{3.26}$$

Konstantou úměrnosti je diferenciální účinný průřez $\sigma(\theta_\mathrm{i}, \phi_\mathrm{i})$:

$$\Gamma b\mathrm{d}b\mathrm{d}\phi = \sigma(\theta_\mathrm{i}, \phi_\mathrm{i})\,\Gamma\mathrm{d}\Omega. \tag{3.27}$$

Protože obě strany rovnice (3.27) odpovídají množství částic rozptýlených za jednotku času, tedy výrazu dN/dt, lze diferenciální účinný průřez považovat za množství částic rozptýlených za jednotku času a vstupního úhlu do prostorového úhlu $d\Omega$:

$$\sigma(\theta_\mathrm{i}, \phi_\mathrm{i}) = \frac{\mathrm{d}N}{\mathrm{d}t\,\Gamma\,\mathrm{d}\Omega} \tag{3.28}$$

Diferenciální účinný průřez lze vyjádřit z rovnic (3.26) a (3.27) jako

$$\sigma(\theta_\mathrm{i}, \phi_\mathrm{i}) = \frac{b}{\sin\theta_\mathrm{i}}\left|\frac{\mathrm{d}b}{\mathrm{d}\theta_\mathrm{i}}\right|. \tag{3.29}$$

Velikost $db/d\theta$ je určena interakční silou, která vyvolává rozptyl. Absolutní hodnota je použita, protože θ obvykle klesá se vzrůstajícím b a $\sigma(\theta_\mathrm{i}a\phi_\mathrm{i})$ jsou kladné veličiny.

Celkový účinný průřez σ_t lze vypočítat integrací σ přes celý prostor

$$\sigma_\mathrm{t} = \int_\Omega \sigma(\theta_\mathrm{i}, \phi_\mathrm{i})\mathrm{d}\Omega = \int_0^{2\pi}\int_0^{\pi} \sigma(\theta_\mathrm{i}, \phi_\mathrm{i})\mathrm{d}\theta\mathrm{d}\phi. \tag{3.30}$$

Veličiny $\sigma(\theta_\mathrm{i}, \phi_\mathrm{i})$ a σ_t závisí na velikosti vzájemné rychlosti částic. V případě centrálně působící síly závisí vzájemný interakční potenciál pouze na vzájemné vzdálenosti částic r. Takový potenciál je izotropní, takže výsledný diferenciální účinný průřez nezávisí na ϕ:

$$\sigma_\mathrm{t} = 2\pi \int_0^\pi \sigma(\theta_\mathrm{i})\mathrm{d}\theta. \tag{3.31}$$

Například Coulombova síla splňuje toto kritérium.

Uvažujme nepohybující se částice rozmístěné s hustotou n_t. Pokud ke srážkám s dopadajícím svazkem částic dochází poměrně zřídka, lze počet částic, které projdou srážkou během průletu oblastí $\mathrm{d}x$ lze vyjádřit jako

$$\mathrm{d}n = -\sigma_\mathrm{tot} n n_\mathrm{t} \mathrm{d}x. \tag{3.32}$$

Při studiu zastavení iontů v materiálu bývá užitečné znát pravděpodobnost, že projektil s energií $E_{\mathrm{i},0}$ předá zasaženému atomu množství energie v rozmezí E_t a $E_\mathrm{t} + dE_\mathrm{t}$. Tato pravděpodobnostní funkce definuje účinný průřez pro přenos energie $\sigma_\mathrm{E}(E_\mathrm{t})$, který je ve vztahu s účinným průřezem $\sigma(\theta_\mathrm{i}, \phi_\mathrm{i})$ jako

$$\sigma_\mathrm{E}(E_\mathrm{t})\mathrm{d}E_\mathrm{t} = \sigma(\theta_\mathrm{i}, \phi_\mathrm{i})\mathrm{d}\theta_\mathrm{i}\mathrm{d}\phi_\mathrm{i}. \tag{3.33}$$

3.4.3 Dynamika elastické srážky

Aby bylo možno určit diferenciální účinný průřez z rovnice (3.29) je nutné najít závislost mezi parametrem rozptylu b a úhlem rozptylu θ_i. Závislost lze stanovit i bez konkrétní znalosti přesné závislosti interakční síly působící mezi částicemi. Za předpoklady centrálně působící síly $\mathbf{F}(r) = F(r)\hat{\mathbf{r}}$ lze využít potenciální energie $U(r)$ díky vztahu

$$\mathbf{F}(r) = -\nabla U(r) = -\frac{\mathrm{d}U(r)}{\mathrm{d}r}\hat{\mathbf{r}}. \tag{3.34}$$

Úhel rozptylu θ_i pak lze zapsat ve tvaru

$$\theta_\mathrm{i}(b, v) = \pi - 2\int_{r_\mathrm{min}}^\infty \frac{b}{r^2}\left[1 - \frac{b^2}{r^2} - \frac{2U(r)}{\mu v^2}\right]^{-1/2} \mathrm{d}r \tag{3.35}$$

kde v je relativní rychlost částic a r_min je nejmenší vzájemná vzdálenost, která je dána vztahem

$$r_\mathrm{min} = b\left[1 - \frac{2U(r_\mathrm{min})}{\mu v^2}\right]^{-1/2}. \tag{3.36}$$

3.4.4 Meziatomový potenciál

Stínící potenciál

Interakce dvou atomových jader je dána coulombovskou potenciální energií

$$U_\mathrm{C}(r) = \frac{1}{4\pi\varepsilon_0}\frac{Z_\mathrm{i} Z_\mathrm{t} e^2}{r}. \tag{3.37}$$

Interakce dvou atomů je však složitější, neboť zahrnuje i vliv elektronového obalu a jeho závislost na vzdálenosti Existují dvě užitečné veličiny, které ohraničují problém a to Bohrův poloměr a_0

$$a_0 = \frac{4\pi\epsilon_0\hbar^2}{m_e e^2}, \tag{3.38}$$

a meziatomová vzdálenosti v krystalu r_0. Bohrův poloměr $a_0 = 0.053$ nm, označuje dosah elektronové slupky atomu. Meziatomová vzdálenost, typicky $r_0 = 0.25$ nm, je vzdálenost mezi mezi dvěma vázanými atomy daná minimem potenciální energie krystalu. Náboj jádra je na vzdálenost $r \gg r_0$ velmi dobře odstíněn elektrony z elektronového obalu. Jak se atomy k sobě přibližují, začnou se elektronové obaly překrývat a může dojít k přitahování atomů a vzniku vazby. V extrémním případě $r \ll a_0$ se jádra stanou vzájemně nejblíže položenými nabitými částicemi v systému. V takovém případě jejich Coulombovská interakce dominuje a potenciální energie je velmi dobře popsána rovnicí (3.37).

Ve střední vzdálenosti $a_0 < r \leq r_0$, má kladná interakční energie, vedoucí na odpudivou sílu, dvě složky (i) elektrostatická odpudivá interakce mezi dvěma jádry (ii) zvýšení energie na základě Pauliho vylučovacího principu.

Ačkoliv přesný popis meziatomové interakce zahrnuje komplikované efekty elektronového obalu, předchozí diskuze ukazuje, že stačí uvažovat rovnici (3.37) upravenou vhodnou limitující funkcí. Ve výsledku je stíněný Coulombovský potenciál popisován tvarem

$$U(r) = \frac{1}{4\pi\varepsilon_0}\frac{Z_\mathrm{i}Z_\mathrm{t}e^2}{r}\chi(r) \tag{3.39}$$

kde χ je stínící funkce. Za ideálních podmínek by $\chi(r)$ mělo jít k nule pro velké vzdálenosti a k jedničce pro malé vzdálenosti.

V podstatě existují dva způsoby vyjádření stínící funkce, (i) jednoduchý statistický a (ii) kvantově-mechanický Hartee-Fockův atomový model.

Thomas-Fermiho statistický model

Statistický Thomas-Fermi (TF) popis předpokládá, že se elektrony chovají jako ideální plyn složený z částic o energii E. Elektrony podléhají Fermi-Diracově statistice a vyplňují potenciálovou jámu v okolí pozitivně nabitého jádra. Tento model evidentně nebere v potaz různé elektronové hladiny.

Přesné řešení TF modelu stínící funkce je obvykle získáno numericky.Avšak pro mnoho aplikací je výhodné mít k dispozici analytické řešení, které přibližně odpovídá TF rovnici. Nejstarší a nejznámější je Sommerfeldův asymptotický výraz:

$$\chi(x) = \left[1 + \left(\frac{x}{a}\right)^\lambda\right]^{-c} \tag{3.40}$$

kde konstanty a, λ a c jsou voleny následujícím způsobem: $a = 12^{2/3}$ a $c\lambda = 3$. Normalizovaná meziatomová vzdálenost $x = r/a_\mathrm{TF}$ je následně modifikována pomocí TF stínícím poloměrem pro srážky mezi atomy

$$a_\mathrm{TF} = \frac{1}{2}\left(\frac{3\pi}{4}\right)^{3/2}\frac{a_0}{Z_\mathrm{eff}^{1/3}} \tag{3.41}$$

kde Z_{eff} je efektivní náboj při interakci dvou rozdílných atomů

$$Z_{\text{eff}} = (Z_{\text{i}}^{1/2} + Z_{\text{t}}^{1/2})^2. \tag{3.42}$$

Sommerfield zjistil, že pro velké x jsou přibližné hodnoty λ a c $\lambda = 0.772$ a $c = 3.886$. Tím dává konečný tvar rovnice (3.43) jako

$$\chi(x) = \left[1 + \frac{x}{12^{2/3}}^{0.772}\right]^{-3.886} \tag{3.43}$$

Další častou používanou aproximací stínící funkce je tvar odvozený Molierem ve formě tří exponenciál:

$$\chi(x) = 7p\exp(-qx) + 11p\exp(-4qx) + 2p\exp(20qx) \tag{3.44}$$

kde $p = 0.05$ a $q = 0.3$. Matematicky jednoduché analytické řešení stínící funkce lze vytvořit při využití inverzní $x = r/a_{\text{TF}}$ s exponentem pro různé rozsahy r/a_{TF}:

$$\chi(r) = \frac{k_s}{s}\left(\frac{a_{\text{TF}}}{r}\right)^{s-1} \tag{3.45}$$

kde $s = 1, 2\ldots$ a k_s je numerická konstanta.

Univerzální meziatomový potenciál - kvantově mechanické odvození

Stínící funkce odvozená za použití kvantové mechaniky vytváří tvar, který je obvykle nazýván jako *univerzální meziatomový potenciál*. Díky práci Zieglera, Biersacka a Littmarka byla odvozena stínicí funkce ve tvaru:

$$\chi_{\text{U}} = 0.1818\exp(-3.2x) + 0.5099\exp(-0.9423x) + 0.2802\exp(-0.4028x) + 0.02817\exp(-0.2016) \tag{3.46}$$

kde je redukovaná dálka x dána jako

$$x = \frac{r}{a_{\text{U}}} \tag{3.47}$$

a a_{U}, univerzální stínící délka, je definována jako

$$a_{\text{U}} = \frac{0.8854a_0}{Z_{\text{i}}^{0.23} + Z_{\text{t}}^{0.23}}. \tag{3.48}$$

Aplikujeme-li meziatomový potenciál se stínící funkcí Eq. (3.45) na rozptylový proces, získáme diferenciální účinný průřez pro rozptyl ve tvaru

$$\sigma_E(E_{\text{i}}) = \frac{C_m}{E_{\text{i}}^m E_{\text{t}}^{1+m}}, \tag{3.49}$$

kde $m = 1/s$ v rovnici (3.45) a konstanta C_{m} je dána jako

$$C_{\text{m}} = \frac{\pi}{2}\lambda_m a_{\text{TF}}^2 \left(\frac{Z_{\text{i}}Z_{\text{t}}e^2}{2\pi\varepsilon_0 a_{\text{TF}}}\right)^{2m} \frac{M_1}{M_2}^2, \tag{3.50}$$

kde λ_{m} je definováno

$$\lambda_{1/3} = 1.309 \quad \lambda_{1/2} = 0.327 \quad \lambda_{0.5} = 0.5. \tag{3.51}$$

3.4.5 Brždění iontů

Because $m_{\text{ion}} \sim m_{\text{target}}$, it leads to considerable energy loss due to elastic collisions. Energy loss for penetration by the distance dx

$$S = -\frac{\mathrm{d}E}{\mathrm{d}x} \tag{3.52}$$

is called **stopping power** or **specific energy loss**. The **stopping cross section** can be defined as:

$$\epsilon = \frac{1}{N}\,\frac{dE}{dx} \qquad \text{or} \qquad \epsilon = \frac{1}{\rho}\,\frac{dE}{dx}, \tag{3.53}$$

where N represent [atoms/m^3] and ρ is the density [kg/m^3]. Sometimes ϵ also represents stopping power.

Obecně lze celkovou ztrátu energie projektilu pohybujícího se v materiálu získat jako součet atomového a elektronového příspěvku:

$$S = S_{\text{n}} + S_{\text{e}}. \tag{3.54}$$

The relative importance of interactions between ions and matter depends on the ion speed, their charge and the atoms of the target

- for $v_{\text{ion}} \ll v_0$, where v_0 is the Bohr velocity of electrons in the atom. Ions will carry their electrons and they tend to be neutralized by electron capture. At these speeds, the elastic collisions dominates and the losses are called**nuclear energy losses**.
- for higher velocities, the importance of nuclear energy losses decreases with a factor of $1/E$ and the inelastic collisions with electrons because important. The collision can result in excitation of electrons of the material and/or excitation of electron in ion electron shells. Above 200 keV/amu, the contribution of nuclear energy losses is typically less than 1 % than electronic one. Between $0.1v_0 \leq v_{\text{ion}} \geq Z_1^{2/3}v_0$ electron collisions are proportional with the velocity ($E^{1/2}$).
- for $v \gg v_0$ the ion charge increases till it completely losses all electrons. The Bethe-Bloch Formula for the electron energy is

  $$\frac{dE}{dx} = NZ_2(Z_1e^2)^2 f(E/M_1), \tag{3.55}$$

  where Z_1 is the ion atomic number.

Jaderné brzdění

Průměrná ztráta energie částice při pohybu o vzdálenost dx lze získat pomocí diferenciálního účinného průřezu pro přenos energie σ_{E}. Ten je definován z rovnice (3.33) jako

$$\langle\frac{\mathrm{d}E}{\mathrm{d}x}\rangle = n\int_{E_{\text{t,min}}}^{E_{\text{t,max}}} E_{\text{t}}\sigma_{\text{E}}\mathrm{d}E_{\text{t}}, \tag{3.56}$$

kde $E_{\mathrm{t,min}}$ a $E_{\mathrm{t,max}}$ jsou minimální, respektive maximální energie předané zasaženému atomu.

Aplikujeme-li diferenciální účinný průřez ze vtahu (3.49), bude účinný průřez pro nukleární zastavování dán

$$S_{\mathrm{n}}(E) = \frac{C_m E^{1-2m}}{1-m}\left[\frac{4M_{\mathrm{i}}M_{\mathrm{t}}}{(M_{\mathrm{i}}+M_{\mathrm{t}})^2}\right]^{1-m}, \tag{3.57}$$

kde C_m je definováno v rovnici (3.50).

Účinný průřez pro jaderné brzdění roste pro nízké hodnoty energie a dosahuje maxima pro jednotky keV pro lehké ionty a stovky keV pro těžké ionty. Lze ho spočítat pro iont s energií E na základě vztahu odvozeného Zieglerem a kolektivemjako

$$\mathcal{S}_{\mathrm{n}} = \frac{8.462 Z_{\mathrm{i}} Z_{\mathrm{t}} S_{\mathrm{n}}(E_{\mathrm{r}})}{(M_{\mathrm{i}}+M_{\mathrm{t}})+(Z_{\mathrm{i}}^{0.23}+Z_{\mathrm{t}}^{0.23})}\mathrm{eVcm}^2/10^{15}\mathrm{atomů}, \tag{3.58}$$

kde E_{r} je redukovaná energie vyjádřená jako

$$E_{\mathrm{r}} = \frac{32.53 M_{\mathrm{t}} E}{Z_{\mathrm{i}} Z_{\mathrm{t}} (M_{\mathrm{i}}+M_{\mathrm{t}}) Z_{\mathrm{i}}^{0.23}+Z_{\mathrm{t}}^{0.23})} \tag{3.59}$$

a $S_{\mathrm{n}}(E_{\mathrm{r}})$ je redukované nukleární brzdění definované jako

$$S_{\mathrm{n}}(E_{\mathrm{r}}) = \frac{\ln(1+1.1383E_{\mathrm{r}})}{2(E_{\mathrm{r}}+0.01321E_{\mathrm{r}}^{0.21226}+0.19593E_{\mathrm{r}}^{0.5})} \qquad \text{pro} \qquad E_{\mathrm{r}} \le 30\,\mathrm{keV} \tag{3.60}$$

nebo

$$S_{\mathrm{n}}(E_{\mathrm{r}}) = \frac{\ln E_{\mathrm{r}}}{2E_{\mathrm{r}}} \qquad \text{pro} \qquad E_{\mathrm{r}} > 30\,\mathrm{keV}. \tag{3.61}$$

Nad 200 keV/amu je příspěvek nukleárního brzděný malý, typicky pod 1 % elektronového brzdění.

Elektronové brzdění

Množství srážek s elektrony, které podstoupí iont při průletu pevnou látkou je obrovské. Zároveň může velmi často docházet ke změně náboje iontu. Je proto velice obtížné popsat všechny možné interakce pro všechny možné stavy iontu. Místo toho se brzdění obvykle vyjadřuje jako průměrná ztráta energie pro různé stavy iontu. Tímto přístupem lze teoreticky určit výsledek s chybou odpovídající několika málo procentům při energiích kolem stovky keV. Nejpřesnější je Betheho formule:

$$S = \frac{4\pi}{m_{\mathrm{e}}c^2}\frac{nz^2}{\beta^2}\left(\frac{e^2}{4\pi\varepsilon_0}\right)^2\left[\ln(\frac{2m_{\mathrm{e}}c^2\beta^2}{I(1-\beta^2)})-\beta^2\right], \tag{3.62}$$

kde v rychlost iontu, c je rychlost světla, $\beta = v/c$, ze je náboj iontu, m_{e} je klidová hmotnost elektronu, $n = N_{\mathrm{A}}Z\rho/A$ je elektronová hustota terče a I excitační potenciál terče.

Pro nižší energie pod přibližně 100 keV na nukleon, bývá obtížnější určit brzdný účinek z teorie

Pro rychlosti iontu v rozsahu $\approx 0.1v_0$ to $Z_{\mathrm{i}}^{2/3}v_0$ je ztráta energie díky elektronům přibližně úměrná $E^{1/2}$, jak odvodil Lindhard a kolektiv.Při vyšších rychlostech $v_{\mathrm{i},0} \gg v_0$ dochází k postupné ztrátě elektronů z obalu iontu až je nakonec zcela ztratí. V takovém případě je ztráta energie úměrná druhé mocnině náboje iontu.

3.4.6 Dolet iontů

Jeden z nejdůležitějších parametrů jakékoliv interakce mezi ionty a pevnou látkou je rozložení hloubky (vzdálenosti), ve které se ionty zastaví. Obvyklé rozložení v amorfní látce iontů majících stejnou energii je přibližně gaussovské. Může proto být obvykle charakterizováno projekcí dráhy R_p a šířkou rozptylu ΔR_p kolem této střední hodnoty, jak je zobrazeno na obrázku 3.11.

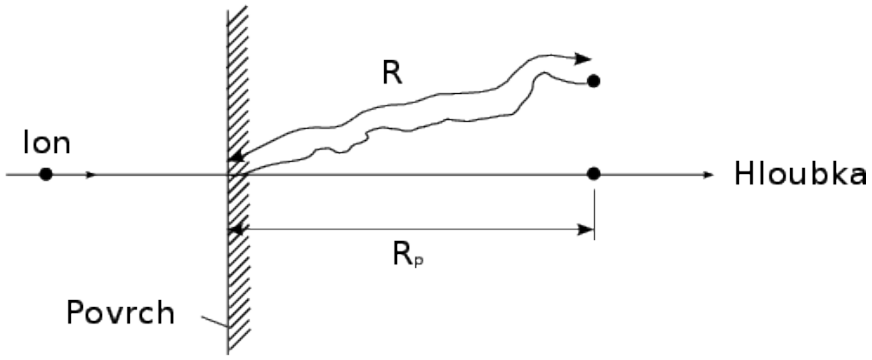

Figure 3.11: Iont dopadající na pevnou látky se v ní pohybuje po dráze R, která vytváří projekci dráhy R_p do původního směru přilétajícího atomu.

3.4.7 Radiační poškození

Přilétající ion s energií odpovídající 100 keV, se v pevné látce zastaví za čas řádově 10^{-13} s díky elektronovému a nukleárnímu brzdění. Během své dráhy v pevné látce vykoná dopadající iont mnoho srážek s atomy pevné látky. Když se jedná o krystalickou látku, může být energie předaná při srážce dostatečná k vyražení atomu z jeho polohy v mřížce.

Takto primárně vyražený atom může následně vyrážet další atomy (sekundární, terciární), čímž vytvoří kaskády atomových srážek. Takovéto srážky vedou k vytvoření prázdných míst, uvěznění atomu mimo mřížku a dalším typům krystalových poruch podél dráhy dopadajícího iontu. *T*ato sekvence mnoha srážek je obvykle nazývána srážkovou kaskádou.

Teorie popisující radiační poškození v pevných látkách je založena na předpokladu, že atom vyražený ze svého místa v krystalu buď iontem, nebo jiným odskočeným atomem musí během srážky získat určitou minimální energii. *D*islokační energie E_d je energie kterou musí atom získat, aby byl vyražen z mřížky.

3.4.8 Termální ohřev

Během srážkové kaskády postupně nastane situace, kdy vyražené atomy vyšších řádů již nebudou mít dostatek energie, aby vyrazily další atomy z jejich poloh v mřížce. Další srážky s atomy pevné látky tak pouze způsobí rozvibrování zasažených atomů s velkou amplitudou výchylky. Tyto vibrace se postupně přenáší na další atomy a energie je rozložena do vibrace mřížky, tedy tepla.

Po přibližně 10^{-12} s je dosažen stav termodynamické rovnováhy, kdy se rozdělení vibračních energie začne blížit Maxwell-Boltzmanově rozdělení. Tato fáze srážkové kaskády se nazývá termální ohřev a může trvat i několik pikosekund, než dojde k poklesu na původní teplotu.

3.4.9 Rozprašování

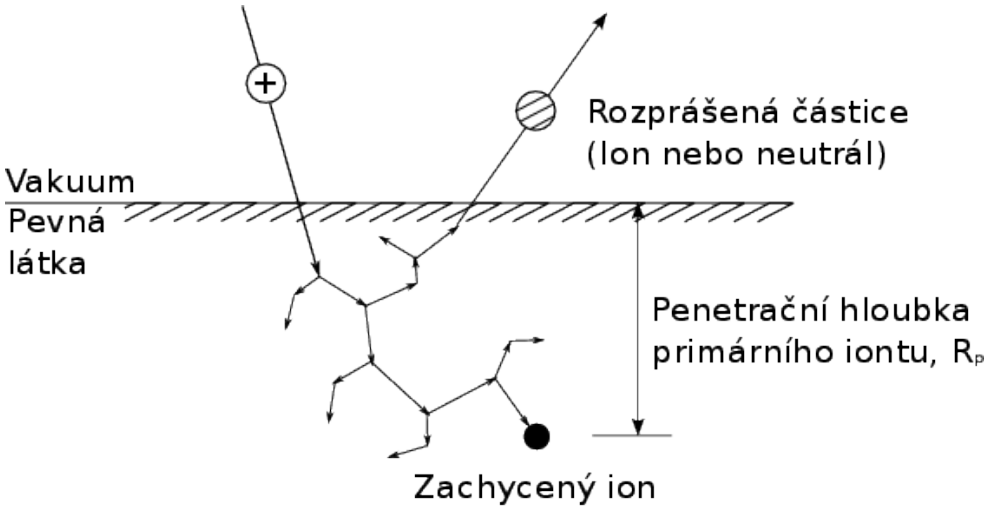

Figure 3.12: Rozprašování

Výtěžnost Y popisuje, kolik atomů je vyraženo během rozprašovací události. Celková výtěžnost je pak definována jako průměrný počet rozprášených atomů připadající na jeden dopadající atom.

Celkové chování atomů terče po dopadu částice lze rozdělit do pěti rozdílných skupin podle E_i, Z_i a M_i, Z_t a M_t. V lineární kaskádní teorii předává počáteční iont energii atomům v mřížce, které jsou v klidu. Produkuje tak velké množství rychlých atomů, které následně produkují další pomalejší atomy. Vzniká tak izotropická kaskáda. Přibližně za $1–5\times10^{13}$ s po dopadu iontu již energie na hranici kaskády klesne pod limitní energii nutnou k vyražení dalšího atomu (přibližně 10 eV). Kaskáda tak zanikne rozptýlením energie do vibrací mřížky. Použijeme-li tuto teorii, lze výtěžnost spočítat pomocí analytického vztahu.

$$Y(E_\mathrm{i}, \theta_\mathrm{i}) = \frac{K_\mathrm{it}}{U_0} S_\mathrm{n}(E_\mathrm{i}/E_\mathrm{it})\, f(\theta_\mathrm{i}), \tag{3.63}$$

kde U_0 je velikost potenciálového valu na povrchu (v eV), K_it a E_it jsou škálovací konstanty závislé na chemickém složení terče a dopadajícím iontu, $S_\mathrm{n}(E_\mathrm{i}/E_\mathrm{it})$ je redukovaný účinný průřez pro jaderné brzdění, ($\epsilon = E_\mathrm{i}/E_\mathrm{it}$ je redukovaná energie) a $f(\theta_\mathrm{i})$ je funkce popisující sklon, pod nímž došlo k nárazu.

3.4.10 Secondary ion-electron emission

According to the adiabatic principle, heavy ions are not efficient for transferring energy to light electrons to provide ionization. This general statement can be referred to the direct electron

emission from solid surfaces induced by ion impact.
The secondary electron emission coefficient γ (electron yield per ion) becomes relatively high only at very high ion energies exceeding 1 keV. Although the secondary electron emission coefficient γ is low at lower ion energies, it is not negligible and remains almost constant at ion energies below the kilovolt range.

$$\gamma = \frac{i_\mathrm{e}}{i_\mathrm{i}}. \tag{3.64}$$

Total γ coefficient is the sum of

$$\gamma = \gamma_\mathrm{p} + \gamma_\mathrm{k}, \tag{3.65}$$

where γ_p is the potential emission and γ_k for the kinetic one.

Iont blížící se k povrchu je reprezentován potenc. jámou ⇒ dojde k tunelovému přechodu e^- z kovu na prázdnou valenční hladinu v iontu ⇒ e^- přejde na nižší hladinu a přebytek energie předá dalšímu e^-, který je emitován. Tento jev je základem tzv. neutralizační spektroskopie.

The **Penning mechanism of secondary ion-electron emission**, also called the potential mechanism: the ion approaching the surface represents a potential well ⇒ dojde k tunelovému přechodu e^- z kovu na prázdnou valenční hladinu v iontu ⇒ e^- přejde na nižší hladinu a přebytek energie předá dalšímu e^-, který je emitován. Tento jev je základem tzv. neutralizační spektroskopie.

The electron is extracted because the ionization potential Φ exceeds the work function ϕ. The energy $\Phi - \phi$ is usually large enough to enable the escape of more than one electron from the surface. The **secondary ion-electron emission coefficient** γ can be estimated using the empirical formula:

$$\Phi \geq 2\phi, \tag{3.66}$$

⇒ potential emissions are observed especially when bombarding the surface with ions of inert gases that have high Φ. γ_p is higher for higher ion charge.

Ion-neutralization spectroscopy (INS) is an emission electron spectroscopy. In INS the externally applied agent is a slowly moving positive ion, such as He^+, presented to the solid surface. Near the surface a non radiative, Auger type electronic transition process occurs which simultaneously neutralizes the ion to the ground state of the parent atom and excites a second electron, which may be ejected into vacuum. The kinetic-energy distribution of these ejected electrons contains spectroscopic information concerning the electronic structure in the surface region of the solid.

- When the incoming ions is just outside the metal surface, two electrons in the filled valence band of the metal interact, exchanging energy and momentum.
- One electron, the neutralizing electron, tunnels through the potential barrier into the potential well presented by the ion, and drops to the vacant atomic ground level.
- The energy released in this transition is taken up by the second interacting election which now may have sufficient energy to escape from the metal
- These Auger type transition can take place anywhere within the filled valence band so that the ejected electrons have a range of energies rather than one specific energy. Outside the metal surface the electron energy distribution can be measured quite straightforwardly.

3.5 Penetration depth

Penetration depth is a measure of how deep light or any electromagnetic radiation can penetrate into a material. It is defined as the depth at which the intensity of the radiation inside the material falls to $1/e$ of its original value at (or more properly, just beneath) the surface.
When electromagnetic radiation is incident on the surface of a material, it may be (partly) reflected from that surface and there will be a field containing energy transmitted into the material. This electromagnetic field interacts with the atoms and electrons inside the material. Depending on the nature of the material, the electromagnetic field might travel very far into the material, or may die out very quickly. For a given material, penetration depth will generally be a function of wavelength.

- **photons**
  The huge electromagnetic spectrum covers wavelengths between 10^6 m and 10^{-14} m. If we use the photons for microstructure analysis it is necessary to select a comparable length of radiation comparable with the structure to be analysed $\Rightarrow$ between 10^{-4}–10^{-10} m. Depth of penetration changes with photon energy and the type of material use for analysis:

  - IR radiation: characterization of materials, which is depending of the absorbed wavelengths;
  - VIS radiation: used often to see the surface. Some material are opaque while others are transparent. Even for high reflectivity opaque materials the penetration depth is in order of 50–300 nm.
  - UV radiation: reveals information about the electron distribution for surface atoms. Most substances absorb in this region.
  - X-ray radiation: X-ray penetration is easier to predict than visible radiation. The penetration depth is typically μm. The intensity of radiation which is transmitted through sample thickness d is
    $$I = I_0 \exp(-\alpha d), \tag{3.67}$$
    where I_0 is the intensity of incident radiation and α, the **absorbance**, increases with the atomic number.
  - Gamma (γ) radiation: has energy between 50 keV–50 MeV $\approx 10^{-2}$ nm. Absorbance is governed by the same relation for X-rays, but here α is inversely proportional with the atomic number. Gamma radiation penetrate almost all the laboratory samples.

- **electrons**
  Penetration depth changes significantly with the electron energy and the atomic number of the material:

  - for stainless steel: around one tenth of a μm for energy 10 keV and 2 μm for 30 keV,
  - for energies higher than 10 keV: elements with atomic number under 20 have a penetration depth up to 10 μm while the elements with Z higher than 40 below 2 μm
  - for energies between 0–2 keV: the penetration depth is reduces to 0.4–300 nm

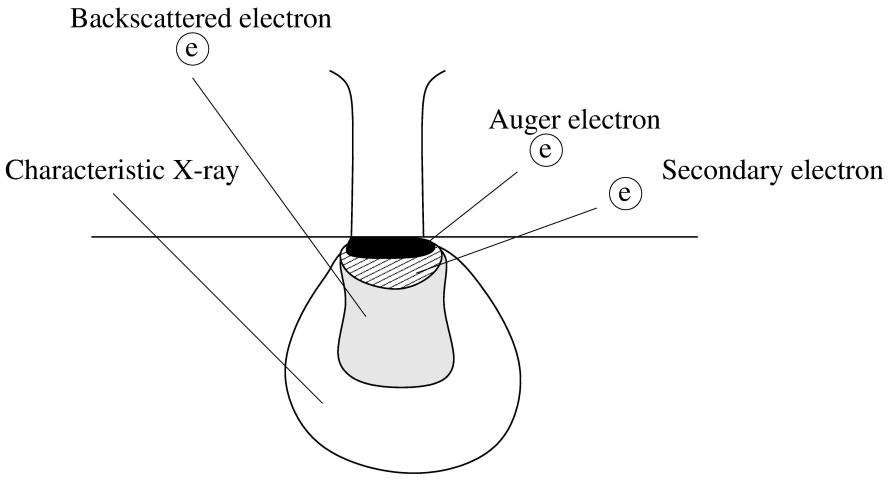

Figure 3.13: Penetration depth for different particles.

- **neutrons**
  Although neutrons are thousand times bigger than electrons, they still have a wave-particle duality. Because they don‘t affect the electron clouds and interact only with the nuclei the penetration depths are larger than those of electrons or X-rays and are in order of few millimetres.

- **protons**
  Protons interactions are similar to electron ones, but some peculiarities can be observed. Being 1836 times the mass of electron, has a higher angular momentum and loses only a small portion of eat at each collision $\Rightarrow$ penetration depth is greater than for electrons. For 2.5 MeV proton, the penetration depth is around 55 μm for carbon and 28 μm for silver; it decreases with the the proton energy and Z of the material.

- **ions/atoms**

  Penetration depth depends on the number of protons in the ion, its energy and the target. For low energies (several eVs) it is reflected from the target and part of its energy is transferred to the surface atom, causing ejection of atoms, ions or clusters. It can also create cascade collisions.
  The range R - the total distance that the ion (projectile) travels in coming to rest, is longer

than the penetration depth x. The **projected range** R_p is defined as the total path length of the projectile with energies $0.002 \leq \epsilon \leq 0.1$ keV measured along the direction of incidence.

$$R_\mathrm{p} = C_1(\mu) M_2 \left[\left(\frac{Z_1^{2/3} + Z_2^{2/3}}{Z_1 Z_2} \right) E \right]^{2/3}, \tag{3.68}$$

where M_2 is the atomic mass of the target , Z is the atomic number while $C_1(\mu)$ is experimentally determined. for projectiles with energies $0.5 \leq \epsilon \leq 10$ keV is

$$R_\mathrm{p} = C_1(\mu) M_2 \left[\left(\frac{(Z_1^{2/3} + Z_2^{2/3})^{1/2}}{Z_1 Z_2} \right) E \right]^{2/3}. \tag{3.69}$$

Ion channelling is possible along crystallographic axes with small critical angles. In this case the penetration depth is substantially increased.

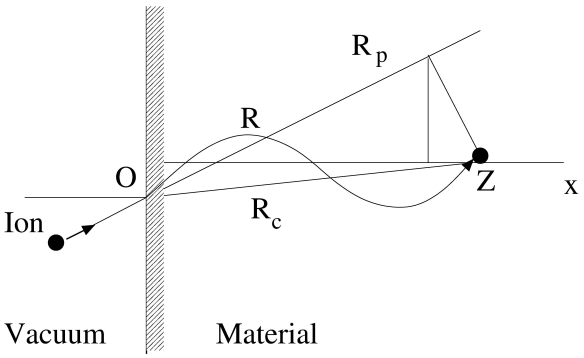

Figure 3.14: Calculation of total distance of ion.

3.6 Material damage

- **photons**
  Regarded in general as the least harmful, the photons will damage the target nevertheless. Damage can occur by heating the target, which depends on the radiant energy, photon flux and the depth of penetration. Moreover X-rays can induce surface oxidation and lasers can burn holes into material. In general the most photon radiation causes very little damage ⇒ it is used at the beginning of target characterization.

- **electrons**
  Although electrons have a dual nature, their weight leads to a relatively large transfer angular momentum if they are accelerated to several hundreds keVs. The resulted damage depends on the heat transferred and the thermal conductivity of the material. For metals and alloys the damage is minimum, but in polymers and oxides the damage is worse. It is possible to cover the surface with a conductive material (usually gold) but the disadvantage is that the composition can not longer be investigated.

- **ions and atoms**
  When atoms and ions penetrate the target, they can react with it or not cause any damage at all (e.g. Ion Scattering Spectroscopy, where ions interact elastically with the target) or they cause significant damage:

  – ejection of atoms form their normal lattice position
  – breaking the bonds (requires 10x more energy)

  For low ion fluxes the damage areas are isolated (the amorphous material is surrounded by intact one) but for high fluxes, the ions create an amorphous layer.

3.7 Resolution

Mean free path determines the depth resolution, which has influence in the spatial one (defined as the perpendicular to the direction of the incident beam). Generally, the spatial resolution is influenced by the beam size and the wavelength.
The image can be obtain by:

- illumination of the sample and use of lens for focusing the reflected or emitted radiation. The spatial resolution depends on the lens system used and the wavelength of emitted or reflected radiation. Optical, X-ray and some ion microscopes are using this method.

- a narrow beam is directed on the sample and absorbed or reflected radiation is detected. The sample surface is scanned by a narrow beam. In this case the spatial resolution depends in the wavelength, beam size and the scattered radiation in the sample. Most of the equipment are using electrons and ions.
  Nowadays, laser microscopes are used for sample characterization.